Viscous Current-Induced Forces

Vladimir U. Nazarov,[1,*] Tchavdar N. Todorov,[2] and E. K. U. Gross[1]
[1]Fritz Haber Research Center of Molecular Dynamics, The Hebrew University of Jerusalem, Institute of Chemistry, Israel
[2]School of Mathematics and Physics, Queen's University Belfast, Belfast, United Kingdom

(Received 11 March 2024; accepted 7 June 2024; published 11 July 2024)

We study the motion (translational, vibrational, and rotational) of a diatomic impurity immersed in an electron liquid and exposed to electronic current. An approach based on the linear response time-dependent density functional theory combined with the Ehrenfest dynamics leads to a system of linear algebraic equations, which account for the competing and counteracting effects of the current-induced force (electron wind) and the electronic friction. We find and emphasize the coupling between the center of mass motion and that of the nuclei relative to each other, the feature due to the mediation of the two-body interaction by the environment. The current-induced forces, by means of the dynamic exchange-correlation (xc) kernel $f_{\rm xc}(\mathbf{r},\mathbf{r}',\omega)$, include the electronic viscosity contribution. Starting from the ground state at the equilibrium internuclear distance and applying a current pulse, we observe three phases of the motion: (i) acceleration due to the prevalence of the current-induced force, (ii) stabilization upon balancing of the two forces, and (iii) deceleration due to the friction after the end of the pulse. At lower, but still metallic, electron densities, the dynamic xc contribution to the force significantly affects the acceleration (deceleration) at the first (third) phase of the process. For the Cs density ($r_s \approx 6$ a.u.), this correction amounts up to 40% in the rotation regime.

DOI: 10.1103/PhysRevLett.133.026301

The current densities in atomic wires can exceed those in macroscopic conductors by many orders of magnitude [1]. Current flow in a lightbulb causes heating, light emission, and electromigration [2], leading to the eventual failure of the current-carrying element. So what should we expect in the microscopic world of atomic wires?

This question has prompted intense research into current-driven dynamics in nanoscale conductors for over 25 years, resulting in simulation techniques of great sophistication [3,4]. Of central importance in these studies is the mean force exerted by the current on individual atomic nuclei. Techniques typically rely on the static density functional theory (DFT) or the self-consistent tight binding (TB) method for the calculation of this all important quantity under nonequilibrium open boundary conditions (see Ref. [5] and references therein).

But it is known that static DFT and TB miss key dynamical effects, which have been shown to be of importance for related phenomena, such as electronic stopping [6,7], bulk impurities resistivity [8], and nanoscale conductance [9–12]. These dynamical corrections, akin to electron viscosity [13], have never been investigated for current-induced forces to the best of our knowledge. The aim of this Letter is to bridge this gap.

We develop a formalism based on the frequency-dependent kernel of the time-dependent DFT (TDDFT) [15,16] and its space-nonlocal extensions [17,18], and apply it to the problem of the electron-wind force on impurities in jellium. The upshot is to significantly correct the current-induced forces and the friction effect at metallic electron densities. This viscous correction to the bare wind force is far from being of academic interest alone. When combined with thermal activation, this increase in the wind force can result in very significant changes to impurity electromigration rates. A related phenomenon where these corrections become of central interest are nonconservative forces under current and the waterwheel effect [19], an application we propose to study in the near future.

We consider two classical nuclei of atomic numbers Z_1 and Z_2 at positions $\mathbf{R}_1$ and $\mathbf{R}_2$, respectively, immersed in an otherwise homogeneous electron gas (HEG) of density parameter r_s, where $\bar{n}^{-1} = \frac{4}{3}\pi r_s^3$, $\bar{n}$ is the HEG density (atomic units are used throughout).

Equilibrium configuration.—In the ground state (GS) at the equilibrium internuclear distance, the forces on each nucleus vanish

$$\mathbf{F}_\alpha = -\int \left[\nabla_{\mathbf{R}_\alpha} \frac{Z_\alpha}{|\mathbf{r}-\mathbf{R}_\alpha|}\right] n_0(\mathbf{r};\mathbf{R}_1,\mathbf{R}_2)\,d\mathbf{r} - \nabla_{\mathbf{R}_\alpha} \frac{Z_\alpha Z_\beta}{|\mathbf{R}_\alpha - \mathbf{R}_\beta|} = \mathbf{0}, \qquad \alpha = 1,2, \qquad \beta = 2,1, \quad (1)$$

where $n_0(\mathbf{r};\mathbf{R}_1,\mathbf{R}_2)$ is the nuclear-position-dependent GS electronic density.

Time-dependent perturbation.—We apply to the equilibrium state a weak external electric field

$$\delta\mathbf{E}_{\rm ext}(t) = \delta\mathbf{E}_{\rm ext}(\omega)e^{-i\omega t}. \quad (2)$$

In the anticipation of our results and to justify the following analysis, we note that we will seek for the charge-density response of our system to the perturbation (2), calculate forces exerted on nuclei, and solve equations of motion. We will do this in three different ways: (i) within the full theory, i.e.,

including both the static and dynamic xc through the spatially and temporally nonlocal $f_{\rm xc}(q,\omega)$, (ii) including the static xc only through $f_{\rm xc}(q,\omega=0)$, and (iii) within the random phase approximation (RPA), i.e., setting $f_{\rm xc}(q,\omega)=0$. By the comparison of the results we will elucidate the role of the dynamic xc (viscosity) effects (see Figs. 2–5).

To *first order* in the perturbation (2), the current density induced in the system is

$$\delta j_{{\rm ind},i}(\mathbf{r},\omega)=\frac{c}{i\omega}\int\hat{\chi}_{ij}(\mathbf{r},\mathbf{r}',\omega)\left[\delta E_{{\rm ext},j}(\omega)+\sum_{\gamma=1}^{2}(\delta\mathbf{R}_\gamma(\omega)\cdot\nabla')\nabla'_j\frac{Z_\gamma}{|\mathbf{r}'-\mathbf{R}_\gamma|}\right]d\mathbf{r}', \tag{3}$$

where i and j are Cartesian indices (summation over the repeated index j is implied). $\hat{\chi}_{ij}(\mathbf{r},\mathbf{r}',\omega)$ is the tensorial *current* density response function [20], in which a parametric dependence on $\mathbf{R}_{1,2}$ is implied. $\delta\mathbf{R}_\gamma(\omega)$ is the displacement, to first order in $\delta\mathbf{E}_{\rm ext}(\omega)$, of the nucleus γ from its equilibrium position. The two terms in the square brackets in Eq. (3) stand for the bare external field and that of the Coulomb charges of the displaced nuclei, respectively.

Based on Eq. (3), in Sec. I of Supplemental Material [21], we show that the electric field due to the dynamical redistribution of electrons is

$$\delta\mathbf{E}_e(\mathbf{r},\omega)=\frac{\omega^2}{\omega^2-\omega_p^2}\delta\mathbf{E}_{\rm ext}(\omega)+\frac{1}{\omega^2-\omega_p^2}\nabla\int\frac{1}{|\mathbf{r}-\mathbf{r}''|}[\chi(\mathbf{r}'',\mathbf{r}',\omega)-\chi(\mathbf{r}'',\mathbf{r}',0)](\delta\mathbf{E}_{\rm ext}(\omega)\cdot\nabla')V_0(\mathbf{r}')d\mathbf{r}'d\mathbf{r}''$$
$$+\nabla\int\frac{1}{|\mathbf{r}-\mathbf{r}''|}\chi(\mathbf{r}'',\mathbf{r}',\omega)\left[\sum_{\gamma=1}^{2}(\delta\mathbf{R}_\gamma(\omega)\cdot\nabla')\frac{Z_\gamma}{|\mathbf{r}'-\mathbf{R}_\gamma|}\right]d\mathbf{r}'d\mathbf{r}'', \tag{4}$$

where $\omega_p=\sqrt{4\pi\bar{n}}$ is the plasma frequency of the HEG,

$$V_0(\mathbf{r})=-\sum_{\gamma=1}^{2}\frac{Z_\gamma}{|\mathbf{r}-\mathbf{R}_\gamma|} \tag{5}$$

is the bare static potential by the nuclei, and $\chi(\mathbf{r},\mathbf{r}',\omega)$ is the *scalar* density response function of TDDFT [15].

The last step is to evaluate the forces on each nucleus. To the first order in the perturbation, they read

$$\delta\mathbf{F}_\alpha(\omega)=Z_\alpha\delta\mathbf{E}_e(\mathbf{R}_\alpha,\omega)-Z_\alpha[(\delta\mathbf{R}_\alpha(\omega)\cdot\nabla_{\mathbf{R}_\alpha})+(\delta\mathbf{R}_\beta(\omega)\cdot\nabla_{\mathbf{R}_\beta})]\nabla_{\mathbf{R}_\alpha}\frac{Z_\beta}{|\mathbf{R}_\alpha-\mathbf{R}_\beta|}$$
$$+Z_\alpha(\delta\mathbf{R}_\alpha(\omega)\cdot\nabla_{\mathbf{R}_\alpha})\nabla_{\mathbf{R}_\alpha}\int\frac{n_0(\mathbf{r})}{|\mathbf{R}_\alpha-\mathbf{r}|}d\mathbf{r},\qquad\beta\neq\alpha. \tag{6}$$

Indeed, the first term on the rhs of Eq. (6) is the field of Eq. (4) at the *unshifted* position of the αth nucleus times its charge. The second and third terms on the rhs stand for the change of the bare force from another nucleus due to the displacements of both of them. The fourth term on the rhs accounts for the change of the force in the potential of the ground-state electronic distribution due to the displacement of the nucleus α. Equations (4)–(6) constitute the main result of our theory. On equal footing, they include current-induced forces and the electronic friction [5,22], and the electron-electron interaction is fully accounted for through the formally exact density response function $\chi(\mathbf{r},\mathbf{r}',\omega)$.

Within the Ehrenfest dynamics, Eqs. (4)–(6) are complemented with the Newton's equations

$$-M_\alpha\omega^2\delta\mathbf{R}_\alpha(\omega)=\delta\mathbf{F}_\alpha(\omega), \tag{7}$$

thus closing the system to be solved to find the displacements $\delta\mathbf{R}_\alpha(\omega)$.

The most challenging element of the described scheme is the determination of the density response function $\chi(\mathbf{r},\mathbf{r}',\omega;\mathbf{R}_1,\mathbf{R}_2)$ of the system of the HEG plus two nuclei in their respective positions. In order to avoid significant computational difficulties while still keeping the essential physics, in the implementation of our theory we resort to the:

Weak electrons-impurity interaction approximation.—This approximation amounts to replacing $\chi(\mathbf{r},\mathbf{r}',\omega;\mathbf{R}_1,\mathbf{R}_2)$ with its HEG counterpart $\chi^h(|\mathbf{r}-\mathbf{r}'|,\omega)$ while, in the equilibrium condition (1), taking

$$n_0(\mathbf{r};\mathbf{R}_1,\mathbf{R}_2)=\int\chi^h(|\mathbf{r}-\mathbf{r}'|,0)V_0(\mathbf{r}')d\mathbf{r}'. \tag{8}$$

Then the force and the potential energy at the given separation d between the nuclei are evaluated to [21], Sec. II

$$F(d)=\frac{Z_1Z_2}{d^2}\left[8\int dq\frac{\chi^h(q,0)}{q^3}(\sin qd-qd\cos qd)+1\right], \quad (9)$$

$$U(d)=\frac{Z_1Z_2}{d}\left[8\int dq\frac{\chi^h(q,0)}{q^3}\sin qd+1\right], \quad (10)$$

where we have Fourier transformed $\chi^h(\mathbf{r},0)$ to the wave-vector variable $\mathbf{q}$. In Fig. 1, the force and the potential energy of Eqs. (9) and (10) are plotted versus the internuclear separation d, for HEG of the density parameter $r_s=2$. We note that, in the weak interaction approximation, the equilibrium separation is independent on the nuclear charges, being a function, via χ^h, of r_s only.

Instead of the external field $\delta\mathbf{E}_{\rm ext}(\omega)$, we introduce the current density $\overline{\delta\mathbf{j}}(\omega)$ in the HEG, as it would be in the absence of the impurity. The two quantities are related by

$$\overline{\delta\mathbf{j}}(\omega)=\frac{i\omega\omega_p^2}{4\pi(\omega^2-\omega_p^2)}\delta\mathbf{E}_{\rm ext}(\omega), \quad (11)$$

which is a consequence of the Drude formula. We, further, introduce the coordinate of the center of mass (c.m.)

$$\delta\mathbf{R}_c(\omega)=\frac{M_1\delta\mathbf{R}_1(\omega)+M_2\delta\mathbf{R}_1(\omega)}{M_c}, \qquad M_c=M_1+M_2,$$

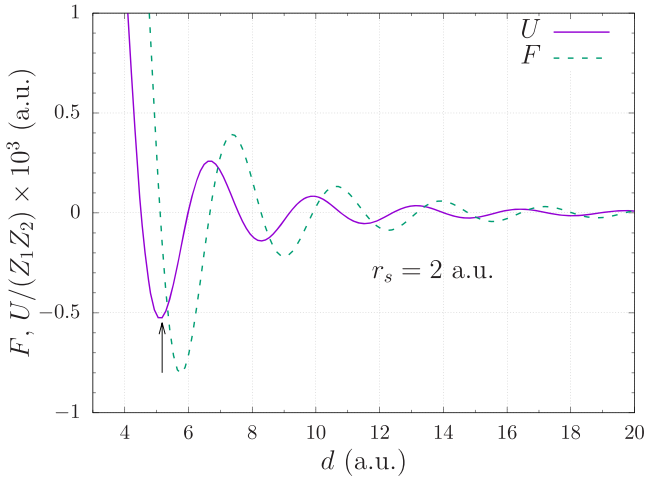

FIG. 1. The potential energy U (10) and the force F (9) versus the distance d between two point charges in the HEG of the density parameter $r_s=2$ a.u. The equilibrium distance between the charges (marked with an arrow) is $d=5.17$ a.u. $\chi^h(q,0)$ used was obtained with Eq. (15) and the MCP07 approximation for $f_{\rm xc}^h(q,0)$ [17].

the relative coordinate

$$\delta\mathbf{R}_r(\omega)=\delta\mathbf{R}_2(\omega)-\delta\mathbf{R}_1(\omega),$$

and the corresponding velocities $\delta\mathbf{V}_c(\omega)$ and $\delta\mathbf{V}_r(\omega)$. This, finally, leads to a system of equations of motion

$$-\omega\delta\mathbf{V}_c(\omega)=-\frac{4\pi(Z_1+Z_2)\omega}{M_c\omega_p^2}\overline{\delta\mathbf{j}}(\omega)+\frac{2}{\pi M_c\omega}\int d\mathbf{q}\frac{\mathbf{q}}{q^4}[\chi^h(q,\omega)-\chi^h(q,0)][Z_1^2+Z_2^2+2Z_1Z_2e^{-i\mathbf{q}\cdot\mathbf{d}}]\left\{\left[\frac{\overline{\delta\mathbf{j}}(\omega)}{\bar{n}}-\delta\mathbf{V}_c(\omega)\right]\cdot\mathbf{q}\right\}$$
$$-\frac{2}{\pi M_c^2\omega}\int d\mathbf{q}\frac{\mathbf{q}}{q^4}[\chi^h(q,\omega)-\chi^h(q,0)][M_1Z_2^2-M_2Z_1^2+Z_1Z_2(M_1-M_2)e^{-i\mathbf{q}\cdot\mathbf{d}}](\delta\mathbf{V}_r(\omega)\cdot\mathbf{q}), \quad (12)$$

$$-\omega\delta\mathbf{V}_r(\omega)=-\frac{4\pi\omega}{\omega_p^2}\left(\frac{Z_2}{M_2}-\frac{Z_1}{M_1}\right)\overline{\delta\mathbf{j}}(\omega)$$
$$-\frac{2}{\pi M_c\omega}\int d\mathbf{q}\frac{\mathbf{q}}{q^4}[\chi^h(q,\omega)-\chi^h(q,0)](\delta\mathbf{V}_r(\omega)\cdot\mathbf{q})\left[\frac{M_1Z_2^2}{M_2}+\frac{M_2Z_1^2}{M_1}-2Z_1Z_2e^{i\mathbf{q}\cdot\mathbf{d}}\right]$$
$$+\frac{2}{\pi\omega}\int d\mathbf{q}\frac{\mathbf{q}}{q^4}[\chi^h(q,\omega)-\chi^h(q,0)]\left\{\left[\frac{\overline{\delta\mathbf{j}}(\omega)}{\bar{n}}-\delta\mathbf{V}_c(\omega)\right]\cdot\mathbf{q}\right\}\left[\frac{Z_2^2}{M_2}-\frac{Z_1^2}{M_1}+\left(\frac{1}{M_2}-\frac{1}{M_1}\right)Z_1Z_2e^{i\mathbf{q}\cdot\mathbf{d}}\right]$$
$$+\frac{2}{\pi\omega}\left(\frac{1}{M_1}+\frac{1}{M_2}\right)\int d\mathbf{q}\frac{\mathbf{q}}{q^4}Z_1Z_2\chi^h(q,0)e^{i\mathbf{q}\cdot\mathbf{d}}[\delta\mathbf{V}_r(\omega)\cdot\mathbf{q}]-\frac{1}{\omega}\left(\frac{1}{M_1}+\frac{1}{M_2}\right)[\delta\mathbf{V}_r(\omega)\cdot\nabla_{\mathbf{d}}]\nabla_{\mathbf{d}}\frac{Z_1Z_2}{d}. \quad (13)$$

While the c.m. motion and the relative one are coupled in Eqs. (12) and (13) we show that the motion in the direction parallel to the impurity's axis and that in the perpendicular direction are independent [21], Sec. III. This allows us to study the two geometries separately. Individual terms in Eqs. (12) and (13) can be attributed a meaning as follows. The first terms on the rhs of both equations are due to the direct field, i.e., the external field (2) screened in HEG. The second terms stand for the combined action of the electron wind and the friction, in Eq. (12), and the friction only in Eq. (13). In the limit $\omega\to0$, a factor $\partial\chi(q,\omega)/\partial\omega|_{\omega=0}$ appears under the integrals. The latter is familiar from the theories of the stopping power for ions and the impurity resistivity [6–8], where it is responsible for energy

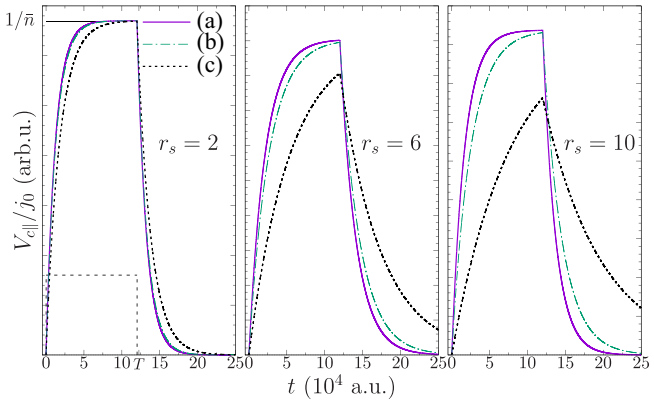

FIG. 2. Velocity of the center of mass of the impurity comprised of a proton and deuteron in HEG of $r_s = 2$ a.u. (left), $r_s = 6$ a.u. (center), and $r_s = 10$ a.u. (right). A rectangular current pulse of the duration T (schematically shown in short-dashed line) is applied in the direction *parallel* to the impurity's axis. At $t < 0$, the system is in its ground state, at the equilibrium separation between the nuclei. The solid (a), dashed (b), and dotted (c) lines show results of calculations by Eqs. (12) and (13) with the use of the rMCP07 xc kernel $f^h_{\rm xc}(q,\omega)$ [18], of its static version $f^h_{\rm xc}(q,\omega=0)$, and in the RPA, $f^h_{\rm xc}(q,\omega)=0$, respectively.

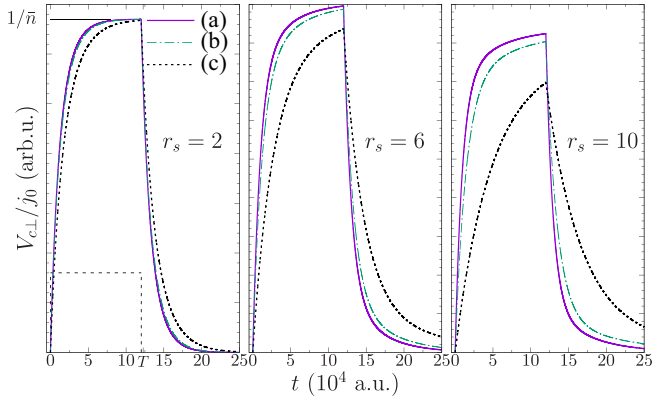

FIG. 3. Same as Fig. 2, but the pulse is applied in the direction *perpendicular* to the impurity's axis.

dissipation. At finite ω, the quantity $\chi(q,\omega)/\omega$ plays the same physical role, although it might be quantitatively influenced according to the magnitude of ω. The third terms are the cross ones, accounting for the c.m. motion dependence on the relative one and vice verse. The last two terms in Eq. (13) stand for the elastic restoring force in the relative motion, as it becomes clear noting that $i\delta\mathbf{V}_r(\omega)/\omega = \delta\mathbf{R}_r(\omega)$. This force gives rise to vibrations shown in Fig 4. When the motion is decomposed into the parallel and perpendicular to $\mathbf{d}$ components, this force survives in the parallel part only [see Ref. [21], Eqs. (S.32') and (S.34')].

Equations (12) and (13) solve our problem in the case of a monochromatic field (2). Furthermore, exploiting the linearity of this approach, by means of the forward and inverse Fourier transforms, we can construct the solution for an arbitrary current pulse $\overline{\delta\mathbf{j}}(t)$. We choose a pulse of rectangular shape

$$\overline{\delta\mathbf{j}}(t) = [H(T-t) - H(-t)]\mathbf{j}_0, \tag{14}$$

where $H(t)$ is the Heaviside's step function and T is the duration of the pulse.

We have conducted calculations using Eqs. (12)–(14) for the impurity comprised of a proton and a deuteron in a HEG of $r_s = 2$, 6, and 10 a.u. In Figs. 2 and 3, we present the time evolution of the velocity of the c.m. of the impurity, in the direction parallel to the axis $\mathbf{d}$ and perpendicular to it, respectively. In Figs. 4 and 5 the same is shown for the relative velocities. The c.m. motion (Figs. 2 and 3) are qualitatively similar in the two geometries. Upon the application of the pulse at $t = 0$, acceleration of the impurity as a whole under the electron wind takes place. The acceleration gradually slows down as the counteracting friction force grows with the increase of the velocity, until the c.m. velocity stabilizes at the value of $\mathbf{j}_0/\bar{n}$, i.e., at the electronic drift velocity. Upon the pulse switching off at $t = T$, the electron wind force vanishes, leading to a fast slowing down of the impurity under the friction force alone.

In Fig. 4, the relative velocity evolution in the direction parallel to the impurity axis is shown. A dominating feature here is the vibrational motion around the equilibrium separation between the two nuclei. The vibrations are, however, of the attenuating amplitudes, after the kicks produced by the pulse switching on and off. This attenuation is due to the coupling between the relative and c.m. motions in Eqs. (12) and (13): when the velocity of the c.m. approaches saturation around the middle of the pulse (see Fig. 2), the electron wind ceases to support the vibrations, while the friction persists, leading to the decay of the oscillations. The frequency and the damping of the oscillations are worked out in Ref. [21] Sec. IV.

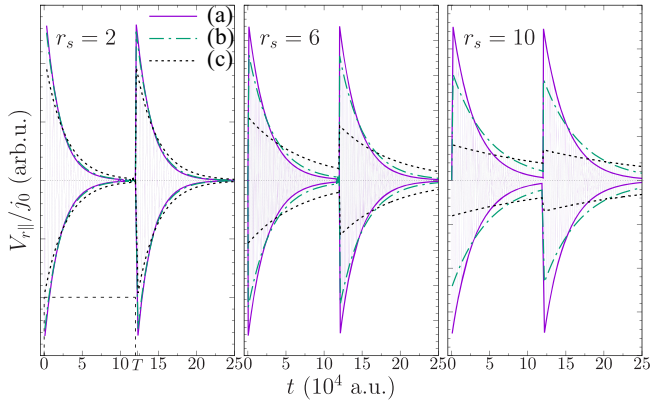

FIG. 4. Same as Fig. 2, but for the velocity of the nuclei relative to each other (vibrations). For visualization, lines circumscribing maxima-minima of the fast oscillations are drawn.

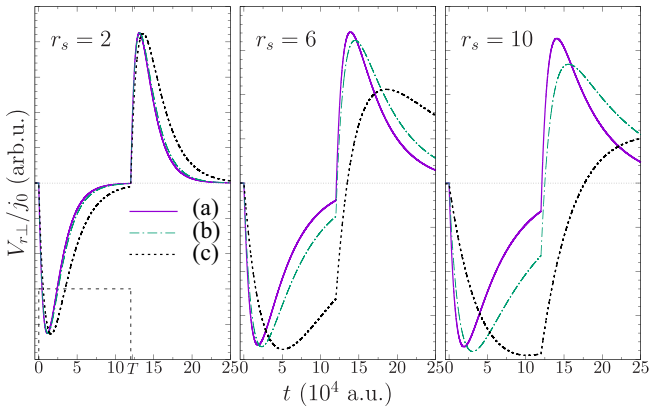

FIG. 5. Same as Fig. 4, but the pulse is applied in the direction *perpendicular* to the impurity's axis (rotation).

Figure 5 also shows the evolution of the relative velocity, but in the geometry with the current perpendicular to the impurity axis. This regime corresponds to the rotation of the impurity around its c.m. Similar to vibrations, the velocity of the rotation quickly increases after the pulse switching on and off, but it falls off in the region of the stabilization. We note that, at the end of the pulse, the direction of the rotation is reversed. This is due to the friction, which is not balanced any more by the electron wind, and which acts in the opposite direction than the latter has acted.

In our theory, a factor of the primary importance is the coupling between the motion of the c.m. of the impurity and that of the nuclei relative to each other. This is due to the mediation by the environment of the electron liquid and it is, obviously, absent in the motion in vacuum. One of the consequences of the coupling is that, in the middle of the pulse duration, when the stabilization of the c.m. velocity is reached, the DC current does not support vibrations and rotation, because the impurity is moving as a whole with the saturation velocity $\mathbf{j}_0/\bar{n}$. However, the pulse switching on or off constitutes kicks on the system, as a result all frequencies get involved, leading to the commencement or resumption of vibrations and rotation which die out afterward due to the friction (see Figs. 4 and 5).

In the determination of $\chi^h(q,\omega)$ in Eqs. (12) and (13), we rely on the linear response TDDFT equality [15]

$$\frac{1}{\chi^h(q,\omega)} = \frac{1}{\chi_s^h(q,\omega)} - \frac{4\pi}{q^2} - f_{\rm xc}^h(q,\omega), \qquad (15)$$

where $\chi_s^h(q,\omega)$ is the Kohn-Sham single particle density response function and $f_{\rm xc}^h(q,\omega)$ is the dynamic xc kernel. While the former is known exactly and analytically by the Lindhard formula [14,23], the knowledge of the latter is limited to approximations. In our calculations we use state-of-the-art spatially and temporally nonlocal xc kernel $f_{\rm xc}^h(q,\omega)$ rMCP07, which is considered accurate at all densities of the fluid phase of HEG [18]. Results are compared with those with the neglect of the temporal nonlocality $f_{\rm xc}^h(q,\omega=0)$ [24], and in the RPA $f_{\rm xc}^h(q,\omega)=0$.

From Figs. 2–5 we conclude that the electronic viscosity, i.e., the temporal nonlocality of $f_{\rm xc}$, significantly influences the motion at lower HEG densities (larger r_s). In the c.m. motion (Figs. 2 and 3), it leads to an increase in the acceleration due to the electron wind at the first phase of the motion, and to a faster deceleration upon the end of the pulse, the latter due to friction. The maximal effect of the viscosity can be observed in the case of the rotational motion (Fig. 5), where, for the Cs density ($r_s = 6$), in the stabilization region (phase II) and at the asymptotic decay of the motion after the end of the pulse (phase III), it leads to the decrease of the velocity by up to 40% (see Ref. [21] Sec. V, for the quantitative comparison).

We anticipate our results to provide a motivation for further research beyond the HEG model. The main challenge on this path is the construction of $f_{\rm xc}(\mathbf{r},\mathbf{r}',\omega)$ for inhomogeneous systems. One of the fruitful methods of doing this is (i) the exploitation of the relation between the tensorial $\hat{f}_{\rm xc}$ of the current density functional theory [20] and the scalar $f_{\rm xc}$ of TDDFT [7,25] and (ii) the use of the local density approximation (LDA) to the tensorial kernel. It is known that such a procedure produced a nonlocal scalar $f_{\rm xc}$ [7,25].

In conclusion, we have studied the motion of a diatomic impurity in an electron liquid under the action of an electronic current. A consistent linear response TDDFT approach combined with Ehrenfest dynamics has been utilized. We have revealed and discussed the consequences of a fundamental property of a composite impurity motion in electron liquid: coupling of the center of mass motion and that of nuclei relative to each other. Our results show that without the inclusion of the electronic viscosity, the electron-wind force and the friction are in general underestimated. For the heavier alkali metals' densities and lower, we find the role of the viscosity of the electron liquid to be of major importance. Fundamental implications for the electromigration theory are envisaged.

This project has received funding from the European Research Council (ERC) under the European Union's Horizon 2020 research and information programme (Grant Agreement No. ERC-2017-AdG-788890). This work was supported also by Queen's University Belfast under the Agility Fund.

*Contact author: vladimir.nazarov@mail.huji.ac.il

[1] T. N. Todorov, J. Hoekstra, and A. P. Sutton, Current-induced forces in atomic-scale conductors, Philos. Mag. B **80**, 421 (2000).

[2] R. S. Sorbello, Theory of electromigration, in *Solid State Physics*, edited by H. Ehrenreich and F. Spaepen (Academic Press, New York, 1998), Vol. 51, pp. 159–231.

[3] J.-T. Lü, S. Leitherer, N. R. Papior, and M. Brandbyge, *Ab initio* current-induced molecular dynamics, Phys. Rev. B **101**, 201406(R) (2020).
[4] M. Stamenova, P. Stamenov, and T. Todorov, Phonon and magnon jets above the critical current in nanowires with planar domain walls, Phys. Rev. Lett. **131**, 206302 (2023).
[5] W. Dou and J. E. Subotnik, Perspective: How to understand electronic friction, J. Chem. Phys. **148**, 230901 (2018).
[6] V. U. Nazarov, J. M. Pitarke, C. S. Kim, and Y. Takada, Time-dependent density-functional theory for the stopping power of an interacting electron gas for slow ions, Phys. Rev. B **71**, 121106(R) (2005).
[7] V. U. Nazarov, J. M. Pitarke, Y. Takada, G. Vignale, and Y.-C. Chang, Including nonlocality in the exchange-correlation kernel from time-dependent current density functional theory: Application to the stopping power of electron liquids, Phys. Rev. B **76**, 205103 (2007).
[8] V. U. Nazarov, G. Vignale, and Y.-C. Chang, Dynamical many-body corrections to the residual resistivity of metals, Phys. Rev. B **89**, 241108(R) (2014).
[9] M. Koentopp, K. Burke, and F. Evers, Zero-bias molecular electronics: Exchange-correlation corrections to Landauer's formula, Phys. Rev. B **73**, 121403(R) (2006).
[10] N. Sai, M. Zwolak, G. Vignale, and M. Di Ventra, Dynamical corrections to the DFT-LDA electron conductance in nanoscale systems, Phys. Rev. Lett. **94**, 186810 (2005).
[11] J. Jung, P. Bokes, and R. W. Godby, Comment on "Dynamical Corrections to the DFT-LDA Electron Conductance in Nanoscale Systems", Phys. Rev. Lett. **98**, 259701 (2007).
[12] N. Sai, M. Zwolak, G. Vignale, and M. Di Ventra, Sai et al. Reply: Phys. Rev. Lett. **98**, 259702 (2007).
[13] For the concepts of the bulk and shear moduli and the viscosity coefficients of electron liquid and their relation to the xc kernel, see Ref. [14].
[14] G. F. Giuliani and G. Vignale, *Quantum Theory of the Electron Liquid* (Cambridge University Press, Cambridge, England, 2005).
[15] E. K. U. Gross and W. Kohn, Local density-functional theory of frequency-dependent linear response, Phys. Rev. Lett. **55**, 2850 (1985).
[16] N. Iwamoto and E. K. U. Gross, Correlation effects on the third-frequency-moment sum rule of electron liquids, Phys. Rev. B **35**, 3003 (1987).
[17] A. Ruzsinszky, N. K. Nepal, J. M. Pitarke, and J. P. Perdew, Constraint-based wave vector and frequency dependent exchange-correlation kernel of the uniform electron gas, Phys. Rev. B **101**, 245135 (2020).
[18] A. D. Kaplan, N. K. Nepal, A. Ruzsinszky, P. Ballone, and J. P. Perdew, First-principles wave-vector- and frequency-dependent exchange-correlation kernel for jellium at all densities, Phys. Rev. B **105**, 035123 (2022).
[19] D. Dundas, E. J. McEniry, and T. N. Todorov, Current-driven atomic waterwheels, Nat. Nanotechnol. **4**, 99 (2009).
[20] G. Vignale and W. Kohn, Current-density functional theory of linear response to time-dependent electromagnetic fields, in *Electronic Density Functional Theory: Recent Progress and New Directions*, edited by J. F. Dobson, G. Vignale, and M. P. Das (Plenum, New-York, 1998), pp. 199–216.
[21] See Supplemental Material at http://link.aps.org/supplemental/10.1103/PhysRevLett.133.026301 for we derive Eqs. (4), (9), and (10); prove the independence of the motion parallel and perpendicular to the impurity's axis; Analytically evaluate the frequencies of vibrations and the corresponding damping constants; Evaluate the relative significance of the viscous correction to the current-induced forces and friction.
[22] W. Dou, G. Miao, and J. E. Subotnik, Born-Oppenheimer dynamics, electronic friction, and the inclusion of electron-electron interactions, Phys. Rev. Lett. **119**, 046001 (2017).
[23] J. Lindhard, On the properties of a gas of charged particles, K. Dan. Vidensk. Selsk. Mat.-Fys. Medd. **28**, 1 (1954).
[24] We note that at $\omega = 0$ the rMCP07 kernel coincides with an earlier MCP07 one [17].
[25] V. U. Nazarov, G. Vignale, and Y.-C. Chang, Communications: On the relation between the scalar and tensor exchange-correlation kernels of the time-dependent density-functional theory, J. Chem. Phys. **133**, 021101 (2010).